ELSEVIER

Contents lists available at ScienceDirect

Construction and Building Materials

journal homepage: www.elsevier.com/locate/conbuildmat



Optimization of experiment methodology based on identification of parameters in concrete drying



Xiaoyan Ma^a, Jérôme Carette^{a,b}, Farid Benboudjema^a, Rachid Bennacer^{a,*}

^a LMT, ENS Cachan, CNRS, Université Paris-Saclay, 94235 Cachan, France

HIGHLIGHTS

- Concrete drying is studied by experiment-numerical-identification coupling approach.
- Accurate and big data-base on mass loss and humidity evolution are obtained.
- Identification of parameters is performed by a LMA minimization in Matlab.
- The optimal experiment protocol duration, number/position of the probes are given.

ARTICLE INFO

Article history: Received 2 October 2019 Received in revised form 26 April 2020 Accepted 1 May 2020 Available online 11 May 2020

Keywords:
Concrete drying
Mass loss
Relative humidity
Parameters identification
Optimal experiment methodology

ABSTRACT

The water transport especially drying process in concrete has a significant influence on its structural durability and stability. However, the inconsistent values of parameters in drying model studies increases the difficulty in predicting the drying process of cementitious materials. In this work, an experimental-numerical-identification coupling approach is developed, based on the non-linear diffusion model, in order to optimize the parameters in drying model, and find out the optimal experiment methodology of concrete drying. Two different geometries of concrete samples are involved, which represent for two drying patterns (prismatic lateral drying and cylindrical radius drying). In the experiment test, both global (mass loss) and local (relative humidity) information are monitored, and the corresponding simulation results are obtained by CAST3M with finite element method. At last, an identification process is performed based on Levenberg-Marquart algorithm, and the optimization combination of parameters are obtained. The analysis of the relative variation of parameters allows to find out the optimization of experiment approach, including test duration and numbers and positions of humidity sensors.

© 2020 Elsevier Ltd. All rights reserved.

1. Introduction

Drying process in concrete is a complex phenomenon. It is a combination result of several factors such as porosity, tortuosity of the material, and the permeability of liquid water, diffusivity of water vapor, as well as interface conditions, ambient temperature and humidity. In addition, the evaporation or condensation of water inside the pore structure add the complexity of the phenomenon. Considered as a porous material, concrete is widely used in constructions in civil engineering, and generally they are subjected to various types of environmental conditions.

During the lifetime of concrete structure, some undesirable pathologies will appear after several years, and eventually resulting in irreversible structure damages [1–5]. Studies shows the

development of these pathologies is closely related to the water distribution in the porous structure, and the loss of free water (non-chemical linked water) from concrete pores, which induces modification on its structural behavior by direct or indirect way [6–8]. Therefore, to obtain the hydric state of concrete is very important to predict the mechanical behavior and durability potential in concrete structures.

However, the moisture transfer process is very complex and affected by several factors, including saturation degree of the void (or water content), the permeability of the porous media, the tortuosity of the concrete pores, surface and ambient conditions [9–12]. In the existing literatures, the most widely used approach to characterize the water content of concrete is to follow weight loss in drying process. This method allows having integral results of water loss but it is not sufficient to have the internal hydrate distribution on different positions. Some indirect methods were developed to test internal humidity to acquire the local water

^b Uni. libre de Bruxelles (ULB), Avenue Franklin Roosevelt 50, 1050 Bruxelles, Belgium

^{*} Corresponding author.

E-mail address: rachid.bennacer@ens-paris-saclay.fr (R. Bennacer).

content. For example, the electromagnetic method [13], X-ray tomography [14], ultrasonic methods [15] and relative humidity probes [16,17]. In addition to the experimental techniques, drying models and numerical approaches were also developed to simulate the drying phenomena [9,10,18,19]. The resolution of a global nonlinear diffusion equation makes it possible to obtain the water content inside the porous structure of concrete.

In the natural environment, the interface is mostly under conventional drying conditions, the mass loss during the drying of specimen are mainly due to the evaporation on the interface between specimen and the ambient, and therefore the pressure gradient induce the transfer of water inside the porous network in the phase of both liquid and vapor. Therefore, in the drying model, coefficients concerning both the permeability of liquid water and diffusivity of water vapor have to be included. Some researchers work on the way to simplify the model by involving only one water transfer coefficient that is a function of saturation degree [20] or the specific water content [21]. Another multiphasic approach proposed to describe the transfer of the gaseous and liquid phases [22,23], in which three constituents are distinguished: liquid water, water vapor and dry air. The moisture transfer is governed by diffusion and permeation equations.

To summarize, the experimental method is the reliable and direct way to follow the moisture state inside concrete. However, the main difficulties include that it is quite time-consuming to follow the slow drying phenomena, and uncertainties and difficulties to trace the inner humidity profile lead to the lack of local hydrate state data (relative humidity). This two main reasons lead to the insufficient database for performing numerical calculation.

The simulation results of mass loss and relative humidity depends highly on the precision of the key parameters in the drying model. However, the suggested parameters in the existing references are not consistent, and it varies for different component ratio of concrete materials, which increases the difficulties in the prediction of drying process in concrete.

Therefore, in this work, we adopted the measurement of both global (mass loss) and local (relative humidity) information to trace the drying process in concrete specimens with two different geometries, to establish a reliable and comprehensive database for the specific concrete material used in this study.

As the experiment process is quite time-consuming, and the monitor for inner humidity is relative difficult, it is necessary to find out the adequate experimental data within the shortest time duration, and to figure out the proper positions and sufficient quantity of sensors to detect relative humidity inside the concrete. In order to achieve this goal, we did calculation on optimization of parameters for different time duration windows and different sensor positions. Taking the experimental results obtained in drying process is considered as reference values, an identification procedure for the parameters involved in the model is performed in this based on finite element modelling updating method using Cast3M and Matlab coupling.

The identification flow chart together with experiment and simulation framework is presented in Fig. 1.

As illustrated in Fig. 1, the protocol could be globally divided into three parts, which are indicated in three different background colors. The first is related to the experimental data obtained in this study; a second part presents the finite element simulation process, and the last part is associated to the minimization algorithm.

2. Experimental protocol

The concrete used in this work is named B11, which has beenstudied by other researchers and properties are mostly known [24]. The hydration reactions can be considered completed, and the self-desiccation phenomenon can be neglected [25,26]. The specimens under drying condition are monitored by regularly recording of mass loss and by continuously recording the internal relative humidity at different positions. Samples are classified into two geometries groups. The first is prismatic with a size of $7 \times 7 \times 28 \text{cm}^3$, which is dried on two lateral faces, and other four surfaces are covered by aluminum paper to prevent any mass exchange during drying process. The other geometry is cylinder of $\varnothing 11 \times 7 \text{cm}^2$, subjected to drying on radius direction and the bottom and top surfaces are covered with aluminum paper. For each geometry, three specimens of the same shape are prepared, two of which are used for mass loss test, and the other one for humidity measurement.

The samples are placed in humidity chamber, which is shown in Fig. 2a. The ambient condition is at temperature of 38 ± 0.5 °C, and relative humidity of $32 \pm 1\%$. Some details of the experimental part can refer to the previous work [27]. Fig. 2a presents the climate chamber with drying specimens inside, and Fig. 2b is the humidity sensor (type FHA646R) used inside the fixed positions in specimen to follow the inner relative humidity value.

The geometries of the specimen are illustrated in Fig. 3. The samples are clarified in two different geometries: cylindrical shape for radius drying and prismatic for lateral drying on two opposite surfaces ($7 \times 7 \, \text{cm}^2$). All the other surfaces are tightly wrapped with aluminum, in order to guarantee the one-dimensional drying. As presented in Fig. 3, the dimension of each geometry and the positions of sensors, A, B or C represents for humidity sensors settled at different positions of the samples. The internal relative humidity data are collected by the probes and mass loss of each sample are regularly recorded manually on weight balance. For the cylinder samples, two sensors are fixed at 1.5 cm and 5.5 cm to the drying surface, respectively, corresponding to position A and B; and for the prismatic samples, three sensors are fixed at the distance of 1.5 cm, 3.0 cm, and 6.0 cm to the drying surface, corresponding to position A, B and C respectively.

3. Drying model and parameters optimizations

The assumption adopted in this drying model is that the moisture transport in the concrete is a combination result of two mechanism: the the permeation of liquid water and diffusion of water vapour. If the concrete porous network is saturated, most of the pore paths (or connected pores) are filled with liquid water, therefore the transport of liquid water will play the predominant role, whereas for a low degree of saturation, the paths for vapour is much more fluent, so the movement of water in the form of vapour diffusion cannot be neglected. The model deduced from mass conservation of water transferred in porous network is presented as Eq. (1).

$$\rho_{l} \left[\Phi \frac{\partial S_{l}}{\partial h} \left(1 - \frac{\rho_{v}}{\rho_{l}} \right) \right] \frac{\partial h}{\partial t} = \text{div} \left[\left(k_{la} \frac{1}{h} \frac{\rho_{l}^{2} RT}{\mu_{l} M_{v}} + D_{eff} \frac{M_{v} p_{vs}}{RT} \right) grad(h) \right]$$
(1)

In which, k_{la} is the liquid apparent permeability, and D_{eff} represents the effective diffusivity of water vapour. These two parameters are the key coefficient controlling the water transfer in the drying model, both of which are variables versus the saturation degree, or the relative humidity. Parameters $\rho_l~(kg\cdot m^{-3})$ and $\rho_v~(kg\cdot m^{-3})$ are the density of liquid water and water vapour, respectively.

 S_l is the saturation degree of liquid, Φ is the porosity of the concrete materials, h represents for the relative humidity, μ_l $(kg \cdot m^{-1} \cdot s^{-1})$ is dynamic viscosity of water, p_{vs} (Pa) is the

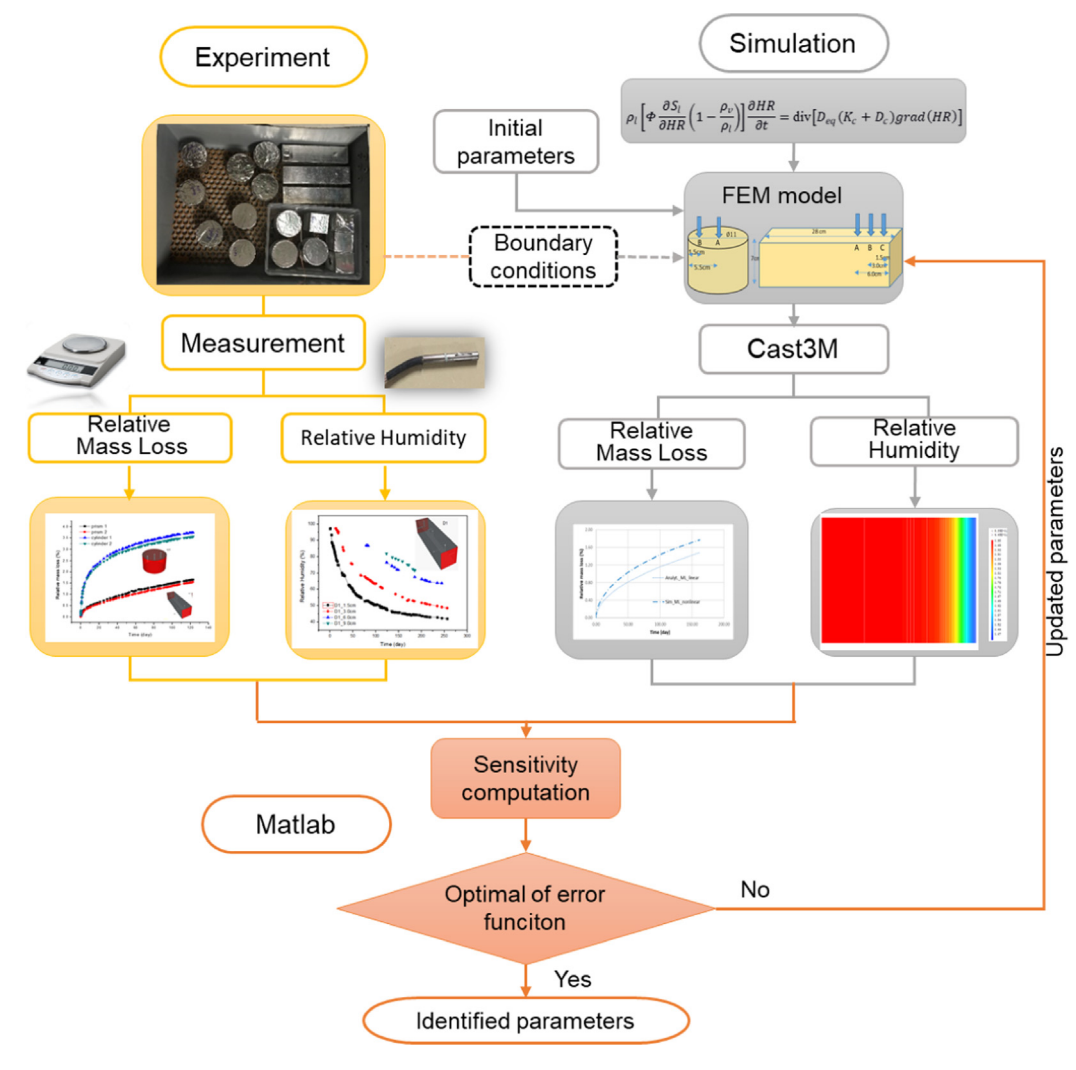


Fig. 1. Identification algorithm flow chart.

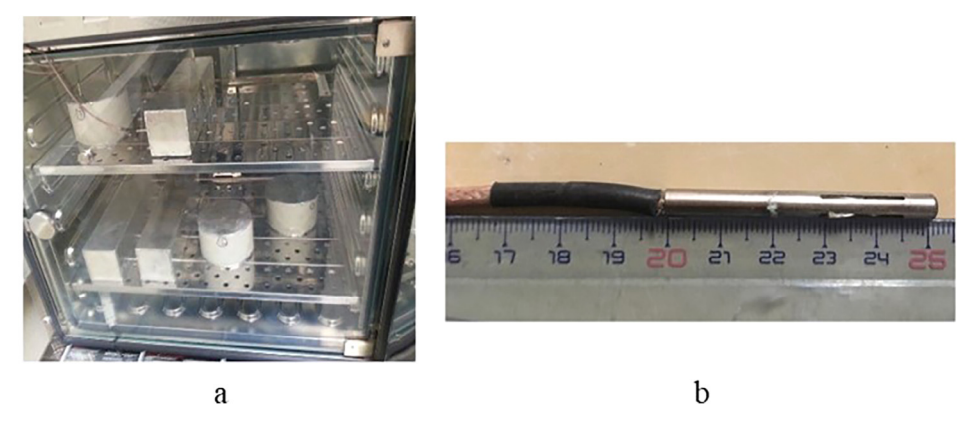


Fig. 2. Experiment devices for drying concrete: a) climatic chamber with specimens; b) humidity sensor.

saturation vapor pressure, $M_{\nu} (kg \cdot mol^{-1})$ is the molecular mass of water vapour,

 $R (8.314J \cdot mol^{-1} \cdot K^{-1})$ is the gas constant.

The right-hand side of the model indicates the moisture distribution on the domain, and the term for equivalent diffusion coefficient contains two mechanisms: the liquid water permeation along the capillaries and the water vapour diffusion through the void.

On the one hand, the liquid permeation flux is deduced from Darcy's law, where k_{la} represents for the apparent permeability of liquid. It is the product of relative permeability k_{rl} and intrinsic permeability of water through the porous structure k_0 , as presented in Eq. (2).

$$k_{la} = k_{rl} \cdot k_0 \tag{2}$$

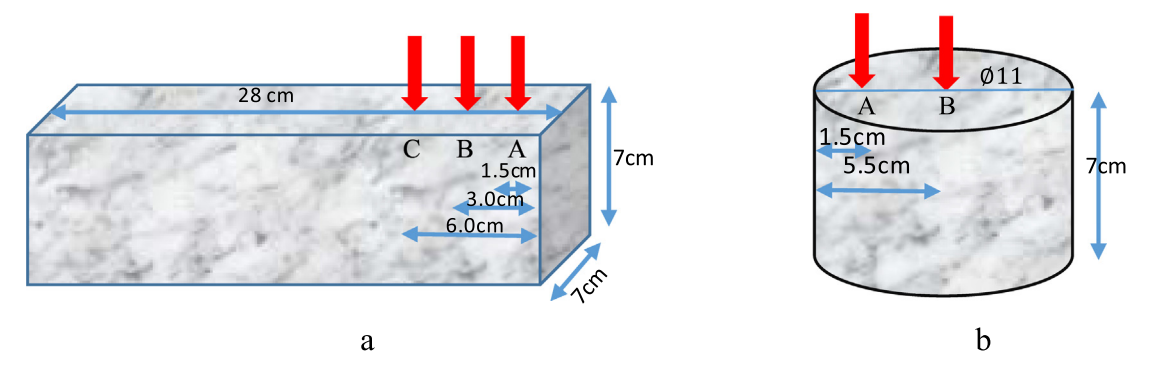


Fig. 3. Schematic diagram of sensors positions for the drying samples of two geometries.

In order to take into account the relationship between water permeability and the saturation degree, the Mualem relationship is presented as Eq. (3) [7], where S_l is the saturation degree of liquid, p_{krl} is a fitting parameter. Moreover, the relationship between the degree of saturation and relative humidity can be described by the Van Genuchten (VG) equation, Eq. (4) [10], where a_{vg} and b_{vg} are two parameters that can be obtained by fitting experimental results of the desorption isotherm for the tested material.

$$k_{rl} = S_l^{p_{krl}} \left(1 - \left(1 - S_l^{\frac{1}{a_{rg}}} \right)^{a_{rg}} \right)^2 \tag{3}$$

$$S_{l} = \left(1 + \left(-b_{vg}ln(hr)\right)^{\frac{1}{1-a_{vg}}}\right)^{-a_{vg}} \tag{4}$$

On the other hand, during the drying process, pores are gradually dehydrated, and the flux of water vapour transfer obeys the Fick's law. The effective diffusion coefficient D_{eff} can be related to saturation degree by the empirical Millington and Quirk (MQ) relationship [18], as expressed in Eq. (5). In which, Φ is the porosity of material, a_{mq} and b_{mq} are two fitting parameters, and D_0 is diffusion coefficient of water in air, which is dependent on temperature, as expressed in Eq. (6), where T_0 (273 K) is the reference temperature and T is the air temperature.

$$D_{eff} = D_0 \cdot \Phi^{a_{mq}} \cdot (1 - S_l)^{b_{mq}} \tag{5}$$

$$D_0 = 2.17 \times 10^{-5} \ \left(\frac{T}{T_0}\right)^{2.88} \eqno(6)$$

In this study, an identification procedure based on experimental data of mass loss and humidity evolution for both the prismatic lateral drying and cylindrical radius drying for seven parameters in the model and equations mentioned above are performed. The identification procedure adopts Finite Element Modelling Updating method (FEMU) [28,29] implemented in CAST3M and Matlab. In the FEMU method, minimisation of an error function is built according to the difference between experimental data and numerical results calculated from CAST3M. As showed previously in Fig. 1, the experimental obtained data is compared with numerical results and finally the minimization algorithm is operated in Matlab.

The methodology applied on both geometries, under the boundary condition of 38 °C temperature, 32% relative humidity, for the test time duration of 16, 40, 80, 120 and 160 days respectively. Iterations of comparison between numerical and experimental data leads to a set of optimized parameters for the corresponding duration of the test. The most comprehensive results of each test group (the longest time duration or the most quantity of humidity sensors) are taken as a reference, in order to have the variation

profile parameters over different test time durations. By this approach, it is practical to figure out the shortest possible test time and the minimal number of humidity sensor that is sufficient for modelling of drying process precisely.

This inverse modelling method depends on a prior knowledge of the drying model and its accuracy to predict the drying process. The error function is given by Eq. (7), which includes experimental data indicated by the *e* exponent, and simulation data indicated by the *s* exponent, as well as results from mass loss measurements, which is indicated by the *ML* index and from relative humidity measurements indicated by the *RH* index. The same approach was applied and detailed explanation can be found in our previous work [26]. This function ensures that several samples or sensors for the same measurement can easily be included independently from one another in the identification process. Finally, the minimization is calculated based on Levenberg-Marquart's optimization method implemented in Matlab.

$$\vec{f} = \sum_{samples} \left[\frac{\vec{C}_{ML}^e}{max(\vec{C}_{ML}^e)} - \frac{\vec{C}_{ML}^s}{max(\vec{C}_{ML}^s)} \right] + \sum_{sensors} \left[\frac{\vec{C}_{HR}^e}{max(100 - \vec{C}_{RH}^e)} - \frac{\vec{C}_{HR}^s}{max(100 - \vec{C}_{RH}^s)} \right]$$

$$(7)$$

The optimized parameters resulting from this procedure are applied in CAST3M as input parameters. The identification process runs until it reaches a criterion based on the average relative increment of the identified parameters increments. If this average variation remains below the limit of 0.3% of the current parameters' values, the identification procedure stops.

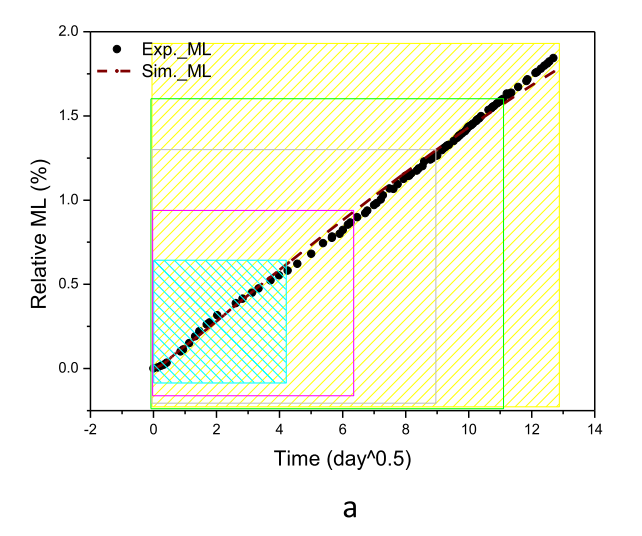
Identification procedure runs firstly only for mass loss of each geometry, followed by mass loss plus humidity data provided by one sensor, then another humidity information is added until all the collected data are applied in the optimization program.

4. Results and analysis

The results are presented in two parts, firstly for the prismatic lateral drying, followed by the results of cylindrical radius drying.

4.1. Results of prismatic lateral drying

The experimental and numerical results of mass loss and relative humidity for prismatic lateral drying is showed in Fig. 4. The relative mass loss in Fig. 4a presents the linear diffusion tendency for lateral drying, and favorable fitting of experiment and numerical are obtained. The relative humidity results at three test points on prismatic sample are presented in Fig. 4b, which indicates that the closer to the drying surface, the higher gradient is humidity



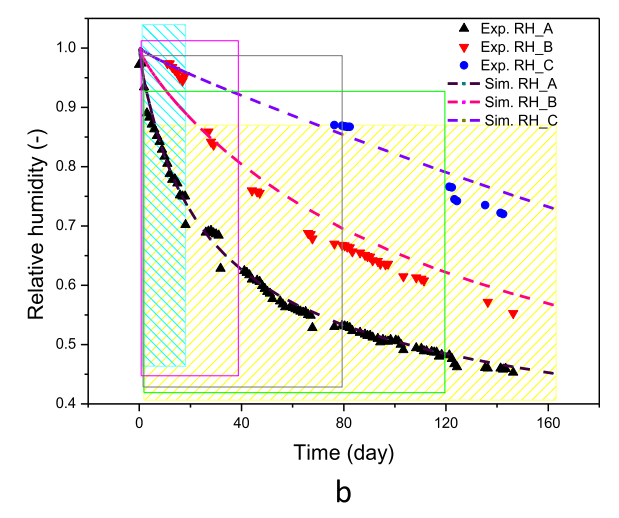


Fig. 4. Experimental and optimized simulation results of a) mass loss, and b) relative humidity. The squares in different colors indicate the varied time duration of 16, 40, 80, 120 and 160 days.

drop. For those sensors that are further from the drying surface, some data is missing, because the continuous high humidity in the beginning period induced condensation of water vapor on the sensor surface. Therefore, condensed liquid water is probably stick on the test point of the sensors, which makes the sensor invalid.

In order to illustrate the time window method, different window duration are shown with the analysis duration of 16, 40, 80, 120 and 160 days in different color squares. The test runs for each time window, with data of mass loss or both mass loss and relative humidity results.

Taking the mass loss window analysis as an example, the optimized parameters for different time durations are listed in Table 1. In this case, the results for 160 days are taken as a reference group, a relative variation of all the other durations with the reference are computed and results are shown in Fig. 5. In order to have a uniform comparison for all the calculation results, 5% of the relative variation is set as a criterion value, as shown in the dashed line in Fig. 5.

Fig. 5 shows the tendency of all the parameters in test containing only mass loss. It is indicated that three of those parameters (intrinsic permeability k_0 , fitting parameters in MQ (a_{nq}) and VG (a_{vg})keep a relative high level (more than 20%) until 90 days, and afterwards, for a longer time duration, these parameters' relative variation decrease rapidly to the reference value. However, in order to include all the parameters variation within the error of 5%, a test duration of at least 150 days is required. This indicates that in prismatic lateral drying, only mass loss data is not sufficient, the relative humidity value is required to allow variation decrease within the predefined errors of 5%. The results of relative variation of parameters for mass loss together with one or two relative humidity data are given by Fig. 6a and 6b, respectively.

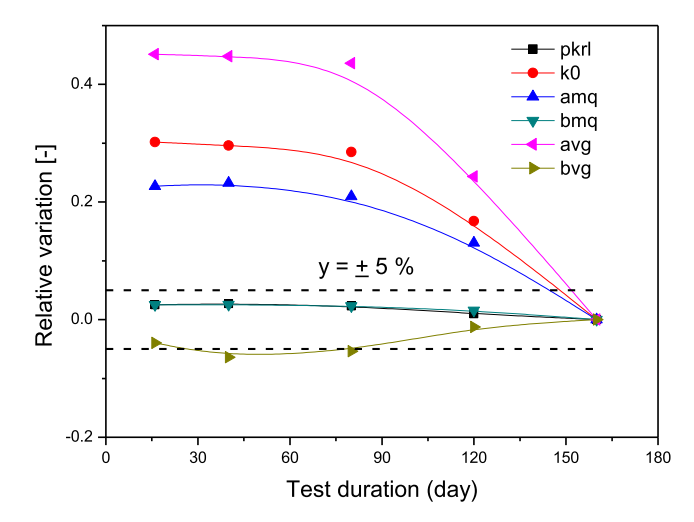


Fig. 5. Relative variation of parameters versus test time duration based on mass loss test result for prismatic lateral drying.

The results including mass loss and one humidity data at position A in Fig. 6a show that except one parameter of a_{vg} in VG, all the other parameters reach in the criterial of 5% when test duration lasts 80 days. When test duration is about 100 days, all the parameters can be included in the defined criterial line of 5%.

The results including mass loss and two relative humidity at position A and B (corresponding to 1.5 and 3.0 cm to the surface) are presented in Fig. 6b. It presents that except the parameter a_{vg} , all the others relative variation decrease to the criterial of 5% at the test duration of 60 days, which is 20 days shorter than that of only one humidity data included. At the test duration of about

 Table 1

 Optimized parameters value for prismatic with mass loss data.

Parameters	Test durations				
	16 days	40 days	80 days	120 days	160 days (Reference)
p_{krl}	0.87019	0.87199	0.8687	0.85738	0.84892
$k_0(10^{-21})$	8.07	8.04	7.97	7.24	6.20
a_{mq}	2.5935	2.6047	2.5566	2.3899	2.1137
b_{mq}	0.740	0.740	0.739	0.734	0.722
a_{vg}	0.24907	0.24842	0.24643	0.21337	0.17161
b_{vg}	0.22387	0.21819	0.22052	0.23016	0.2331

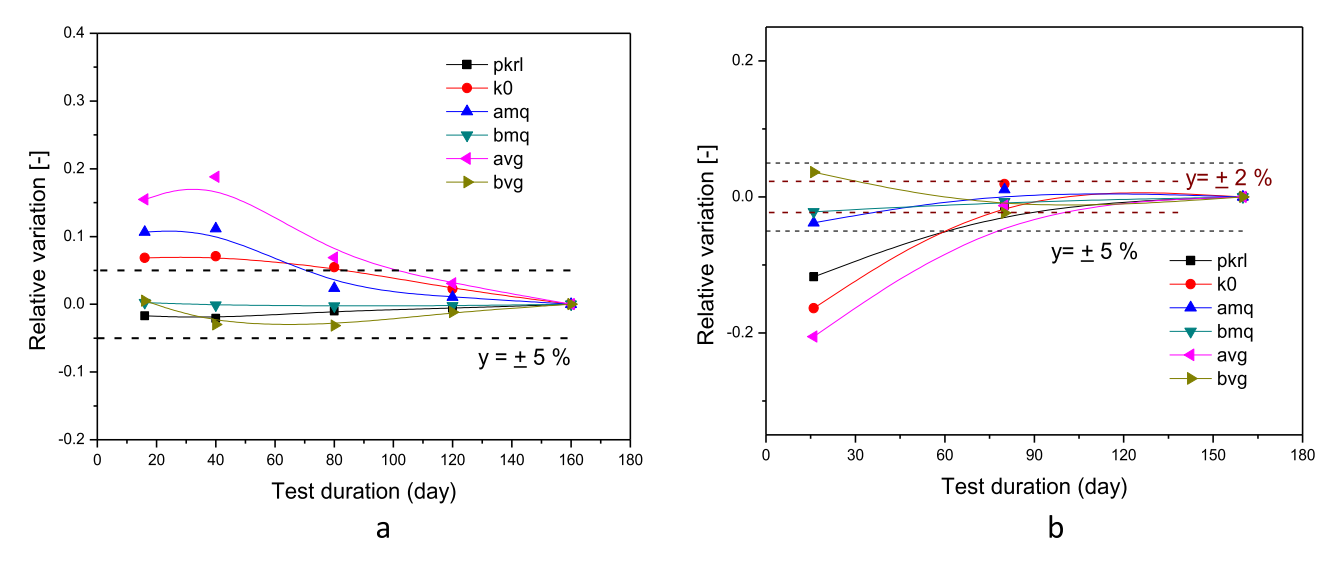


Fig. 6. Relative variation of parameters versus time duration based on a) ML with one RH sensor at position A; and b) ML with two RH points at A and B for prismatic drying.

75 days, all parameters are included in the 5% error lines. In addition, if the same test duration of 100 days is performed, the variation error for two sensors will decline to 2%, which is less than half of the pre-defined critical error of 5%.

An overall comparison between Fig. 5 and Fig. 6 indicates that the relative humidity data contribute to determining parameters, which is positive in improving precision of simulating the humidity profile. Specifically, if one humidity sensor is added in addition to mass loss, the duration for relative variation to reach the criteria error of 0.05 will decrease to 100 days, instead of 150 days, namely 33% of test time is shortened. Besides, a second sensor data will contribute to reducing the test duration to 75 days, which is 25% less of experimental test time in comparison to test with 1 humidity sensor, and 50% less in comparison with test duration of only mass loss. It is convinced that for prismatic lateral drying test, the inner humidity data is necessary to supply for precision prediction of drying modelling and it contributes to save considerable time for the experimental test.

In order to analyze the effect of sensor numbers and positions, we took the identified parameters based on mass loss and three humidity points for a test duration of 160 days as a reference, and the relative variation of six parameters are calculated based

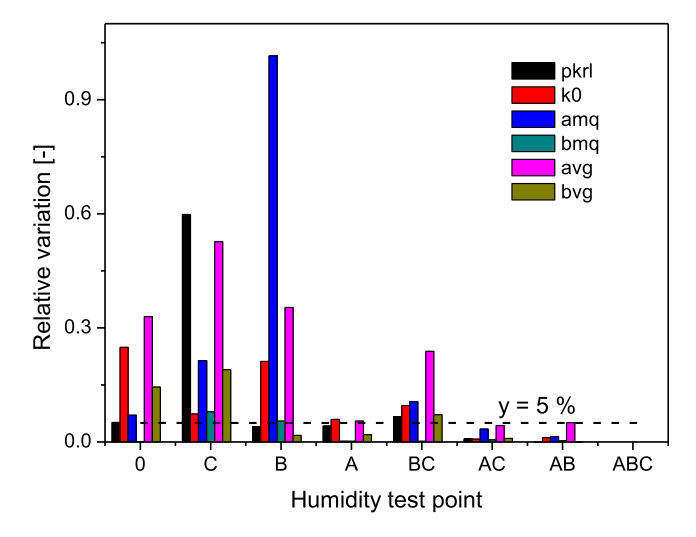


Fig. 7. Effect of sensor positions and combinations of relative variation of parameters for prismatic drying.

on this reference, for different sensor positions and different combinations. Absolute variation values are plotted in Fig. 7 and each color represents for one parameter. The x-axis shows the name (position) or combinations of the sensors in the prismatic geometry as previously illustrated in Fig. 3a.

Although there is no unified trend for all the parameters, the relative variation of parameters roughly decreases with the increase of sensor numbers. When taking combination of three sensors ABC as the reference data, the group of two sensors BC, AC or AB has smaller variation than the group one with only sensor. The exception is sensor A and combination of BC, namely, all the parameters obtained with one sensor of A have a smaller relative variation than the two sensors of combination BC. It indicates that if more sensors data included in drying simulation could increase the precision of parameters, but meanwhile the position and combination of humidity data are also important. If there is only one sensor applied, represented by A, B or C, we found that the position A, which is the closest to the drying surface, is better than the positions that are further to the drying surface. This is due to the higher humidity gradient when the position is closer to the interface exposed to external environment. If two sensors are applied, at least one of them should be the closest to the drying surface. Namely, in addition to this sensor A, add any one more sensor will also slightly improve the precision.

Results between zero humidity sensor (which means only mass loss results are included.) and one sensor represented by C or B, suggested that only one sensor at the far position from drying surface does not contribute to the precision of the parameters, it could also be worse than no humidity sensors. This is because for the position far from the drying surface, the relative humidity changes very slowly and keeps constant high value in the beginning of the drying process. Therefore, parameters go further from the real one to fit with the experimental data. In the meanwhile, another notable reason is that the simulation and identification process is highly dependent on the precision of the tested experimental data. While for the experimental data, the most comprehensive information for humidity is captured in position A, which is the closest to the lateral drying surface, while the farther position B obtained less data and the farthest C recorded the least of the three.

The relative variation criterial value of 5% is also plotted in Fig. 7, and it shows that the data from sensor A and combination of AC or AB is within this line. Namely if two sensors are applied for humidity measurement, the combination of two sensors has to include the one which is most close to the drying surface, other-

wise two sensors could be less precise than one. Nevertheless, the distance in practical is also confined by the size of the sensor probe and technique of the fixing the sensors without destroying the concrete surface.

4.2. Results of cylindrical radius drying

The experimental and simulation results for cylinder geometry test of mass loss and relative humidity at two positions are presented in Fig. 8. The same calculation method with prismatic case is applied to analyze the cylinder radius drying.

It displays in Fig. 8 that unlike the prismatic case, the mass loss evolution is not linear to square root of time any more, but a higher drying rate at the beginning and slow down subsequently, for the curvature effect that the surface area is not constant along the moisture transport direction for the cylindrical radius drying. The drying direction is radial therefore the drying surface which is perpendicular to it is decreasing over time.

Taking the parameters resulted from longest test time duration of 160 days as the reference value, relative variation of parameters for the test of only mass loss is plotted in Fig. 9. It presents that for all the parameters, with increasing the tested time duration windows, tendency of relative variation is decreasing and getting closer to the reference value. It also indicated that the time duration of at least 140 days is necessary to reach a criterial error within 0.05, on condition that the test data is performed only on mass loss.

For the parameter b_{mq} , which is the parameter in MQ equation, the tendency is not so regular, but for all the value, the relative change is below 1%, which is almost negligible in variations. Therefore, it could be considered already reach the relative real value with the reference value.

Results of relative variation for mass loss and one humidity sensor data at position B are shown in Fig. 10.

It is indicated that all the parameters tend to the reference value, which shows similar tendency with test only on mass loss. The gradient is high until almost 80 days, then the rate decrease. This indicates that 90 days can be considered as a criteria that all the parameters relative variation included within a criterial error of 0.05. This is deduced around 50 days in comparison with the results of only mass loss test, meaning that to reach the same level of relative error, 35% of test time is saved if one humidity information is added to mass loss test.

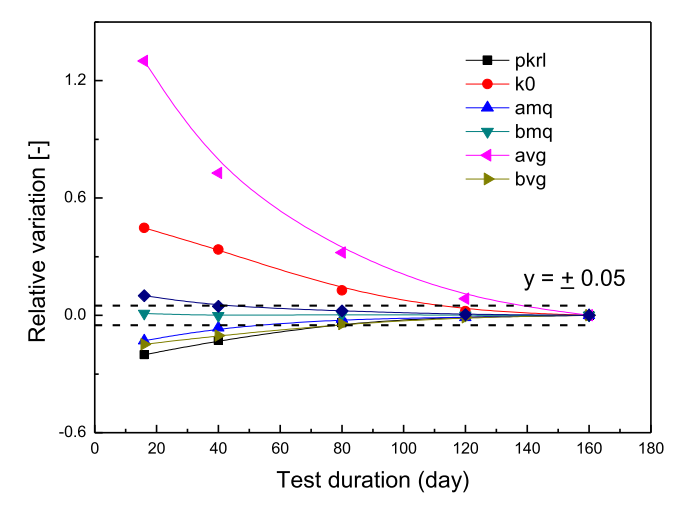


Fig. 9. Relative variation of parameters versus time duration based on mass loss results.

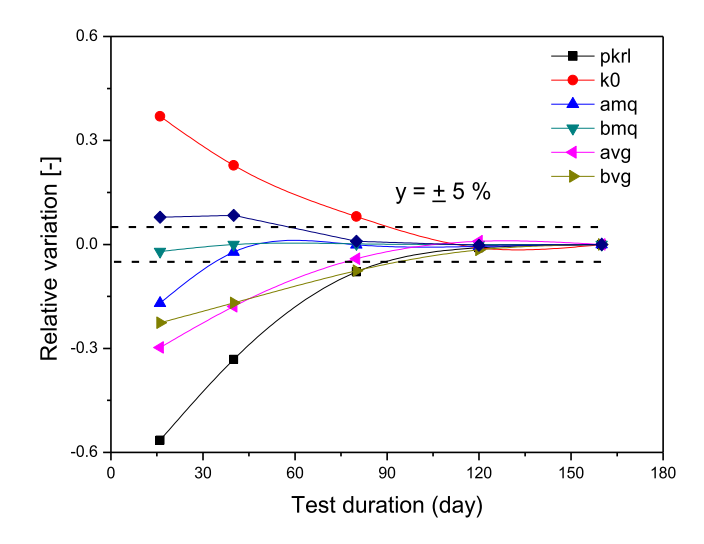
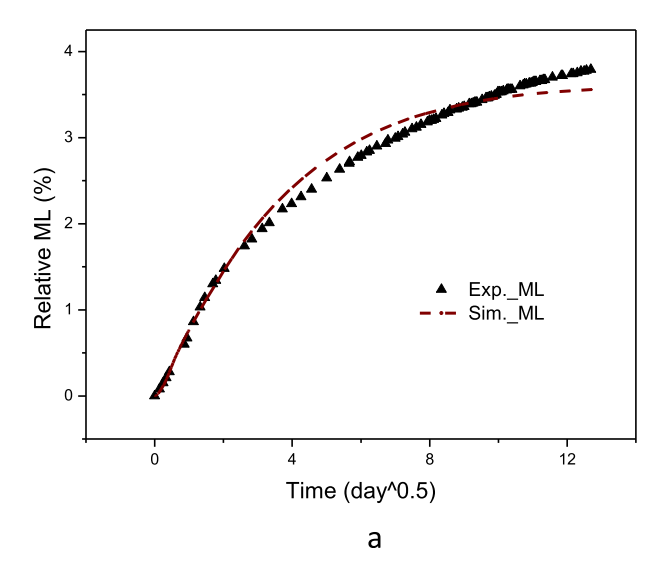


Fig. 10. Relative variation of parameters versus time duration based on ML with RH points at position A for cylinder case.



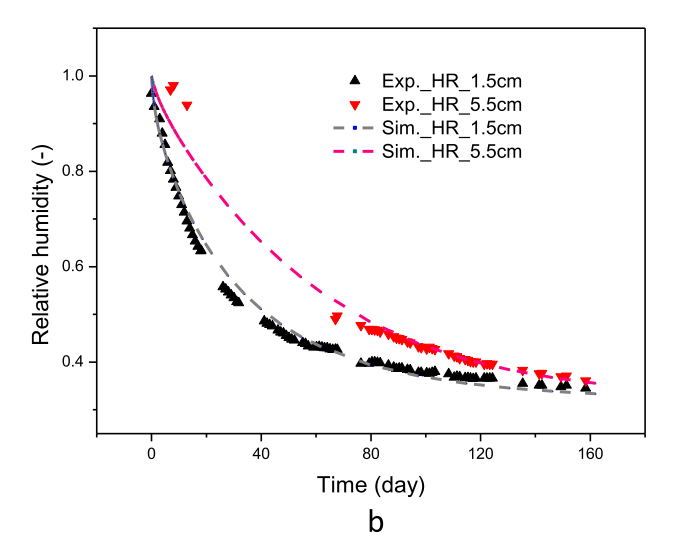


Fig. 8. Experimental and optimized simulation results of a) mass loss, and b) relative humidity, for cylinder radius drying process.

Except the two parameters in MQ equation a_{mq} and b_{mq} , which shows some oscillation phenomena. Nevertheless, for these two parameters, the relative variations is much lower than the others for all the time durations, and both of them are below 1% when time duration is more than 50 days.

Comparing with the test results with only mass loss, we can conclude that if one sensor is added to the test of mass loss, the time duration of criteria relative variation of 0.05 to reference value will decrease from more than140 days to 90 days. To express in another way, if the same time duration of 120 days is applied for the two cases, the relative variation will decrease from 5% to 1%. Therefore, that inner humidity data is necessary to supply for precision prediction of drying modelling and it helps to save considerable time for the experimental duration.

The set of parameters, which is deduced from of mass loss and all the relative humidity of cylinder drying fittings for 160 days, are taken as local reference for analyzing the number of sensors and positions effect on optimized parameters results. The relative variation of parameters for cylinder based on the number of sensors and different positions is shown in Fig. 11.

Taking the results of both sensors as reference value, we can see from the results that all the parameters except the intrinsic permeation k_0 shows a decreasing tendency of relative variations with the increase of sensor test numbers. If there is no value of relative humidity, the relative error could be as large as 50% for some high sensitivity parameters, as parameter used in relative permeation p_{krl} and parameter in van Genuchten equation a_{vg} . It also indicates that for the position at 1.5 cm to the drying surface is better than the position at 5.5 cm, since almost all the parameters show less difference to the reference value. This is reasonable that the position, which is closer to the drying surface, is more necessary because the higher gradient of humidity difference appears closer to the drying interface. This is consistent with the conclusion of prismatic case.

5. Summary and conclusions

In this work, the drying process of concrete with two different drying pattern is monitored by both global and local measurement. An experimental-numerical-identification coupling approach to identify parameters in the drying mechanism of concrete is applied based on a non-linear diffusion model concerning two mechanism:

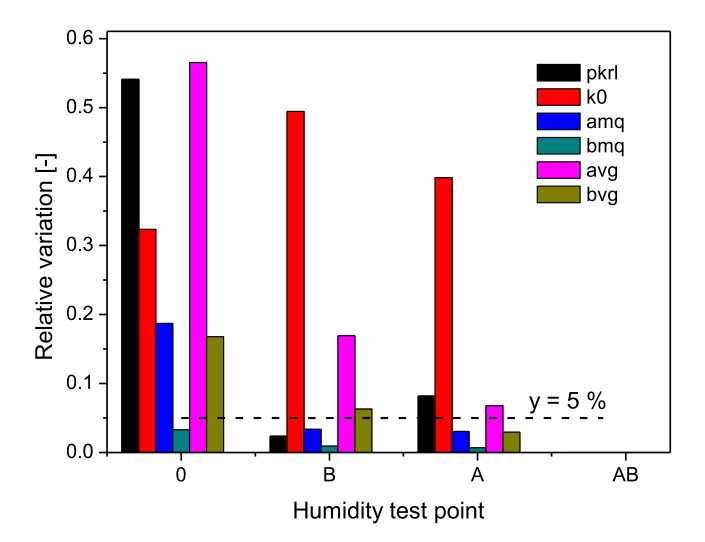


Fig. 11. Effect of sensor numbers and positions on relative variation of parameters for cylinder case.

permeation of liquid water and diffusion of water vapor. The relative variation of optimized parameters for different time duration and different sensor positions are analyzed to acquire the adequate experimental data and best positions of humidity sensors within the shortest time duration.

To be specific, for prismatic lateral drying, results of relative variation of parameters shows that it is necessary to have at least one senor for inner relative humidity profile. The test duration time will decrease with the increase of humidity sensor numbers. A second sensor data will contribute to saving 30% of experimental test time to reach the same level of relative error, and more than 50 of time in comparison to test with only mass loss. If two sensors are applied for the humidity data, one of them has to be at the position that is close to the drying surface, in order to capture the faster variation under the high gradient of humidity.

For the cylinder radius drying, the relative variation of parameters follows roughly an exponential evolution of continuously decreasing to the reference value with the increase of test duration time, and the precision increases with the additional numbers of humidity sensor. There is around 50 test days shortening when there is one sensor information added in comparison with the results of only mass loss test. Two sensors are recommended for a higher precision of the calculation, and one of them has to be as close as possible to the drying surface. The position of closer to the drying position is better than the center positions, since almost all the parameters gives less difference to the reference value.

In short, to follow and predict the humidity profile inside concrete, the test of only mass loss is not sufficient to get precise parameters to apply in the drying model, at least one sensor information is necessary to predict the desorption profile. If only one sensor is applied in detecting the inner relative humidity evolution, the position, which is closer to the drying surface, is better than further ones. Nevertheless, in reality, it is also confined by the fixing technique of the sensors.

CRediT authorship contribution statement

Xiaoyan Ma: Methodology, Writing - original draft, Formal analysis. **Jérôme Carette:** Conceptualization, Methodology. **Farid Benboudjema:** Conceptualization, Validation, Methodology, Writing - review & editing, Formal analysis. **Rachid Bennacer:** Methodology, Software, Writing - review & editing, Formal analysis.

Declaration of Competing Interest

The authors declare that they have no known competing financial interests or personal relationships that could have appeared to influence the work reported in this paper.

Acknowledgements

We thank to the China Scholarship Council (CSC) for its financial support to the first author, No. 201608120052.

References

- [1] H. Wang, J.E. Gillott, Mechanism of alkali-silica reaction and the significance of calcium hydroxide, Cem. Concr. Res. 21 (1991) 647–654.
- [2] J. Zhang, D. Hou, Y. Han, Micromechanical modeling on autogenous and drying shrinkages of concrete, Constr. Build. Mater. 29 (2011) 230–240.
- [3] S. Diamond, Delayed ettringite formation processes and problems, Cem. Concr. Compos. 18 (3) (1996) 205–215.
- [4] C. Sa, F. Benboudjema, M. Thiery, J. Sicard, Analysis of microcracking induced by differential drying shrinkage, Cem. Concr. Compos. 30 (10) (2008) 947–956.
- [5] H. Min, W. Zhang, X. Gu, Effects of load damage on moisture transport and relative humidity response in concrete, Constr. Build. Mater. 169 (2018) 59–68.

- [6] Z. Bažant, Y. Xi, Drying creep of concrete: constitutive model and new experiments separating its mechanisms, Mater. Struct. 27 (3) (1994) 3–14.
- [7] J.K. Kim, C.S. Lee, Prediction of differential drying shrinkage in concrete, Cem. Concr. Res. 28 (7) (1998) 985–994.
- [8] B.D. Liu, W.J. Lv, L. Li, P.F. Li, Effect of moisture content on static compressive elasticity modulus of concrete, Constr. Build. Mater. 69 (2014) 133–142.
- [9] Y. Mualem, A new model for predicting the hydraulic conductivity of unsaturated porous media, Water Resour. Res. 12 (3) (1976) 513–522.
- [10] M.A. Van Genuchten, Closed-form equation for predicting the hydraulic conductivity of unsaturated soils, Soil. Sci. Soc. Am. J. 44 (5) (1980) 892–898.
- [11] F.R. Troeh, J.D. Jabro, D. Kirkham, Gaseous diffusion equations for porous materials, Geoderma 27 (3) (1982) 239–253.
- [12] Q. Huang, Z. Jiang, X. Gu, W. Zhang, B. Guo, Numerical simulation of moisture transport in concrete based on a pore size distribution model, Cem. Concr. Res. 67 (2015) 31–43.
- [13] Z. Sbartaï, S. Laurens, J. Rhazi, J. Balayssac, G. Arliguie, Using radar direct wave for concrete condition assessment: Correlation with electrical resistivity, J. Appl. Geophys. 62 (2007) 361–374.
- [14] I. Jerjen, L. Poulikakos, M. Plamondon, P. Schuetz, T. Luethi, A. Flisch, Drying of porous asphalt concrete investigated by X-Ray computed tomography, Phys. Proc. 69 (2015) 451–456.
- [15] Z. Sbartaï, D. Breysse, M. Larget, J. Balayssac, Combining NDT techniques for improved evaluation of concrete properties, Cem. Concr. Compos. 34 (2012) 725–733
- [16] J. Granja, M. Azenha, C. de Sousa, R. Faria, J. Barros, Hygrometric assessment of internal relative humidity in concrete: practical application issues, J. Adv. Concr. Tech. 12 (2014) 250–265.
- [17] J. Zhang, J. Wang, Y. Han, Simulation of moisture field of concrete with presoaked lightweight aggregate addition, Constr. Build. Mater. 96 (2015) 599-614.
- [18] R. Millington, J. Quirk, Permeability of porous solids, Trans. Faraday Soc. 57 (1961) 1200–1207.

- [19] Z. Zhang, M. Thiery, V. Baroghel-Bouny, Investigation of moisture transport properties of cementitious materials, Cem. Concr. Res. 89 (2016) 257–268.
- [20] Z. Bažant, L. Najjar, Drying of concrete as a nonlinear diffusion problem, Cem. Concr. Res. 1 (5) (1971) 461–473.
- [21] B. Perrin, V.B. Bouny, L. Chemloul, Méthodes de détermination de la diffusivité hydrique de pâtes de ciments durcies, Mater. Struct. 31 (4) (1998) 235–241.
- [22] V. Baroghel-Bouny, M. Mainguy, T. Lassabatere, O. Coussy, Characterization and identification of equilibrium and transfer moisture properties for ordinary and high-performance cementitious materials, Cem. Concr. Res. 29 (8) (1998) 1225–1238
- [23] M. Thiery, V. Baroghel-bouny, N. Bourneton, G. Villain, C. Stéfani, Modélisation du séchage des bétons, Revue Européenne de Génie Civil 11 (5) (2007) 541– 577.
- [24] A. Hilaire, Etude des déformations différées des bétons en compression et en traction, du jeune au long terme : application aux enceintes de confinement, (2014) PhD Thesis, ENS Cachan.
- [25] M. Briffaut, F. Benboudjema, J.-M. Torrenti, G. Nahas, Numerical analysis of the thermal active restrained shrinkage ring test to study the early age behavior of massive concrete structures, Eng. Struct. 33 (4) (2011) 1390–1401.
- [26] J. Carette, F. Soleilhet, F. Benboudjema, X. Ma, G. Nahas, K. Abahri, A. Darquennes, R. Bennacer, Identifying the mechanisms of concrete drying: an experimental-numerical approach, Const. Build. Mater. 230 (2020) 117001.
- [27] X. Ma, A. Darquennes, F. Benboudjema, G. Nahas, R. Bennacer, Study of drying and Imbibition cycles in concrete: effects of sample shape and boundary condition, Int. Conf. Mater. Energy Tianjin, 2017.
- [28] J. Neggers, J.P.M. Hoefnagels, M.G.D. Geers, F. Hild, S. Roux, Time-resolved integrated digital image correlation, Int. J. Numer. Meth. Eng. 103 (3) (2015) 157–182
- [29] Jose Pujol, The solution of nonlinear inverse problems and the Levenberg-Marquardt method, Geophysics 72 (4) (2007) 1–16.